International Journal of Innovative Computing, Information and Control
Volume **9**, Number **12**, December **2013**

ICIC International ©2013 ISSN 1349-4198
pp. 4863–4874

IMAGE ENLARGEMENT USING PYRAMID WINDOW KERNEL BASED ON LOCAL IMAGE DATA

I Komang Somawirata, Keiichi Uchimura and Gou Koutaki

Department of Computer Science and Electrical Engineering
Graduate School of Science and Technology
Kumamoto University
2-39-1 Kurokami Kumamoto 860-8555, Japan
kmgsomawirata@navi.cs.kumamoto-u.ac.jp

Received December 2012; revised May 2013

Abstract. *This paper proposes image enlargement using pyramid window kernel method (PWK). The PWK method consists of three steps. The first step is providing the size for the target image. The size of target image can be in different ratios and shapes. Then perform back-transformation to the source image to obtain the corresponding coordinate for filling pixel. The second step is getting 3×3 sample pixel in surrounding the back-transformation point and calculates one pixel using the pyramid. The reducing 3×3 sample pixel window to 2×2 size must consider the positions of back-transformation point on the source image, and one pixel is calculated from 2×2 window using linear weighting. The third step fills the corresponding coordinate in the target image. The test result for scale factors equal to four on Lena, Boat, Baboon, Peppers, Butterfly, Zebra and Dolphin shows that the peak signal-to-noise ratio (PSNR) values of PWK are always better than the comparison method. As well as the evaluation using correlation shows the PWK method has good results. This indicates, the image enlargement using PWK method produces good image quality. The computation time of PWK method is faster than that of comparison methods. The experimental result in different ratios using PWK is also presented.*

Keywords: Pyramid, Window, Enlargement

1. Introduction.

Resizing of the images, especially for enlarging the image is very important in image processing. It is used for photography, video rendering and electronic display devices. Currently, the variety of displays sizes has been presented. High-resolution displays have been widely used in many areas such as high-definition televisions, mobile devices and smart phones [1, 2]. These require a good enlarging image method. The enlarging image method is used to generate high-resolution (HR) images.

The classic problem of image enlargement is that the image tends to look rough and blurry, which leads to lower image quality. Another problem in the image enlargement method is that it is difficult to be implemented for different ratios and shapes of the target image size. Therefore, it needs to create a new image enlargement method that produces a high-quality performance and is easy to be applied in the varying sizes of display.

Furthermore, the application of the proposed method is used to video rendering. Video rendering requires an image enlargement method that can resize the image to the desired display size. In order to change the image size it is necessary to preserve the contents of an image while changing its size [3, 4, 5, 6]. By more creatively applying our method, an image enlargement with proportional content can be generated by enlarging the selection area in the image.

Many algorithms have been developed to produce high resolution images, one of which is hybrid algorithm [7]. Hybrid algorithm is a combination between wavelet and neural network. The genetic fuzzy system is implemented for image interpolation with limitation of margin [8]. The kernel is developed for interpolation and maintains details of image margin. The margin is calculated by using information combination of fuzzy logic local gradient and genetic algorithm learning. These algorithms [7, 8] are very complex and require learning before being used to make the high-resolution image.

Image enlargement method without learning process was conducted in [9]. Image enlargement uses linear weighing to obtain one pixel interpolation, that is called as WLE method. The WLE method explains the interpolation in three different positions: interpolation between two horizontal pixels, interpolation between two vertical pixels, and interpolation between four pixels. The WLE method is easy to be computed, so it is very convenient to be applied in hardware. However, WLE method does not provide a good result, especially for enlarging an image on scale factor greater than two. Reverse Diffusion Interpolation (RDI) with Partial Differential equation is used to obtain the value of the highest gradient direction to produce the Reverse Diffusion process [10]. The weakness of RDI method does not use the filtering process in homogeneous regions, and no extra parameter is needed to characterize an edge. Meanwhile, the image enlargement based on regularity on the geometric uses covariance-based adaptive interpolation, especially in edge area and the pixels near of edge [11]. They use bilinear interpolation for non edge pixels. This method is called NEDI. The complexity mathematical formulation in NEDI methods causes the long computing time.

Pyramid method is a multi-level technology of image scaling, especially for enlarging or minimizing image. Pyramid method has been used in digital image processing application [12, 13, 14, 15, 16]. The Pyramid Spatial Multi Scale (PSMS) implements the bilinear interpolation for scaling method. The pyramid method is also developed in [17], and the proposed study is about the multi-resolution and image reconstruction of long distance sensing. Fuzzy Adapted Linear Interpolation (FALI) algorithm for enlarging image is presented in [18]. Fuzzy method is used to calculate weight and determine the local gradient. FALI algorithm is implemented on three scaling methods such as bilinear, bicubic and bicubic splines.

In order to overcome the drawback of the previous method, a new method is proposed in this research paper. In our study, image enlargement method is based on pyramid method. The pyramid method is used to obtain the importance pixel for the sample pixel kernel. We make simple formulation to obtain weight value by using linear curve.

Pyramid method has contributed an important role in image enlargement or HR images. In our study, the improvement and efficiency process were conducted by applying the pyramid method to reducing the 3×3 sample pixel kernel. We call this method as the pyramid window kernel (PWK). The image enlargement of PWK method is based on the filling pixel process. The PWK method is also easy to be implemented on image retargeting. Target image size not only in the same ratio, but also in the different ratios can be handled. In addition, PWK can be implemented in the variety of shapes and sizes of the target image.

2. Pyramid Enlargement Method.

Pyramid method is conducted gradually using bilinear weighing scaling method [19]. Figure 1 illustrates pyramid step process. It also shows staging image enlargement using scale factor (S'_n) until the desirable image size is obtained. On each step of the image enlargement process, the reference data will be taken from a lower image position in the pyramid. There are several image hidden layers on

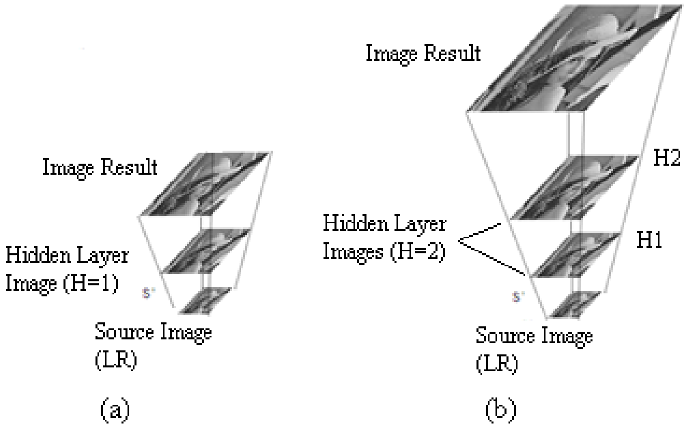

FIGURE 1. Image enlargement using pyramid method

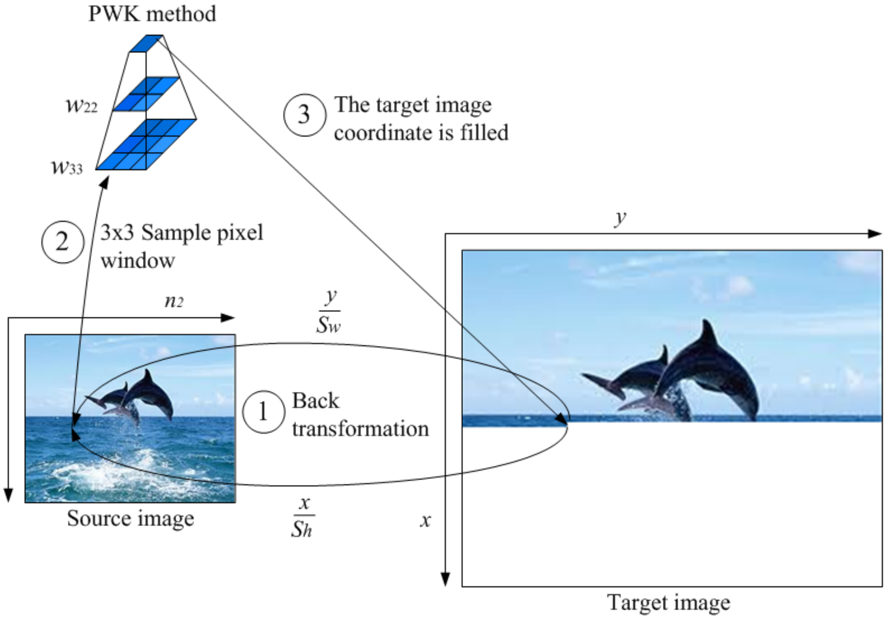

FIGURE 2. Image enlargement using PWK

pyramid method (H_n). The last step is the image result of the pyramid. Hidden layers image is a layer between the source image (LR) and the image result.

Pyramid layers exist if the enlargement values are bigger than two ($S > 2$). If S is bigger than 2, thus the number of the hidden image layers is $H = S - 2$ and the enlargement on each layer is $S'_n = (S/(S-1) + S'_{n-1})$ per layer.

3. **Proposed Method.** This paper introduces image enlargement using windows kernel based on filing pixel. Figure 2 shows the steps of image enlargement using PWK. This method consists of three steps. The first is back transformation from target image coordinate to source image coordinate. The second finds the sample pixel and applies PWK. The sample pixel 3×3 window is reduced into 2×2 window size, and one pixel is calculated using the linear weighting method. The last fills the target image coordinate.

The window kernel reduction was similar with a pyramid. We call it as the Pyramid Window Kernel (PWK). The kernel is an algorithm to reduce sample pixel 3×3 window to the 2×2 window size. Detailed explanation of each step is presented in the subsection below.

3.1. **Target image size.** Generally, a new matrix size of target image $f_T(x, y)$ is obtained by multiplying the width and height of source image $(f_s(n_1, n_2))$ with scale factors for height (S_h) and width (S_w). A new matrix size $f_T(x, y)$ can be written in Equation (1). Matrix size for the new image $(f_T(x, y))$ is still vacant. The pixel for filling empty matrix is obtained from the calculation using PWK.

$$f_T(x, y) = \begin{vmatrix} a_{1,1} & a_{1,2} & a_{1,3} & \cdots & a_{1,MS_w} \\ a_{2,1} & a_{2,2} & a_{2,3} & \cdots & a_{2,MS_w} \\ a_{3,1} & a_{3,2} & a_{3,3} & \cdots & a_{3,MS_w} \\ \vdots & \vdots & \vdots & \ddots & \vdots \\ a_{NS_h,1} & a_{NS_h,2} & a_{NS_h,3} & \cdots & a_{NS_h,MS_w} \end{vmatrix} \tag{1}$$

where N and M are respectively for the height and width size of matrix $f_s(n_1, n_2)$. S_h and S_w are scale factors for height and width, respectively. Meanwhile, a new matrix size for $f_T(x, y)$ is $(NS_h \times MS_w)$.

In contrast, the scale factor can also be calculated by dividing the size of target image with source image size. If the size of target image is $\hat{N} \times \hat{M}$, then the scale factor for the height and width can be obtained by Equations (2) and (3), respectively.

$$S_h = \frac{\hat{N}}{N} \tag{2}$$

$$S_w = \frac{\hat{M}}{M} \tag{3}$$

3.2. **Windows pyramid.** We were able to determine the sample pixel coordinate in the source image $f_s(n_1, n_2)$ using Equations (4) and (5).

$$n_1 = \lceil i_x \rceil \tag{4}$$

$$n_2 = \lceil i_y \rceil \tag{5}$$

wherein $\lceil\rceil$ is rounding-up to the close integer value.

The back transformation points in the source image for i_x and i_y can be found by Equations (6) and (7).

$$i_x = \frac{x}{S_h} \tag{6}$$

$$i_y = \frac{y}{S_w} \tag{7}$$

wherein x and y are respective for the height and width on target image coordinate, which will be filled.

Next, we retrieve the sample pixel data of neighbouring coordinate, by the sized 3×3 such as shown in Equation (8).

$$w_{33}(i, j) = \begin{vmatrix} f_s(n_1 - 1, n_2 - 1) & f_s(n_1 - 1, n_2) & f_s(n_1 - 1, n_2 + 1) \\ f_s(n_1, n_2 - 1) & f_s(n_1, n_2) & f_s(n_1, n_2 + 1) \\ f_s(n_1 + 1, n_2 - 1) & f_s(n_1 + 1, n_2) & f_s(n_1 + 1, n_2 + 1) \end{vmatrix} \tag{8}$$

where $w_{33}(i, j)$ is sample pixel 3×3 window size with $i = j = 1, 2, 3$ and $f_s(n_1, n_2)$ is source image (LR).

Reducing sample pixel 3×3 window size to 2×2 must consider the positions of back transformation point in the source image. There are three conditions in reducing the sample pixel 3×3 window to 2×2 by the kernel based on back transformation point.

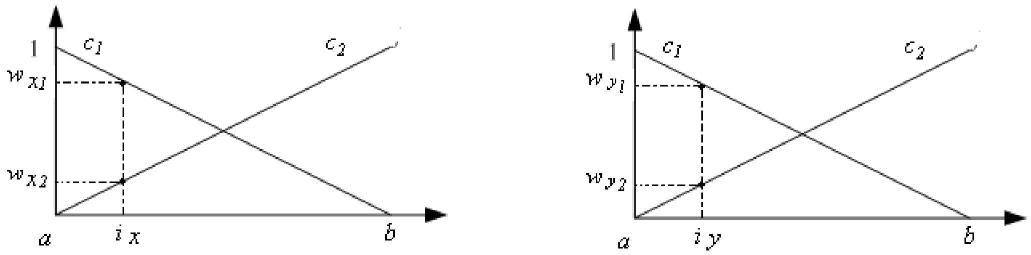

(a) Linear curve for x weight

(b) Linear curve for y weight

FIGURE 3. Linear curve for weight

1. The first condition, if the back transformation point for i_x is an integer and i_y is fraction, then the pixel in the element matrix w_{22} window is shown as Equation (9).

$$w_{22}(i,j) = \begin{vmatrix} w_{33}(2,2) & w_{33}(2,3) \\ \dfrac{w_{33}(3,2)+w_{33}(3,3)}{2} & \dfrac{w_{33}(1,2)+w_{33}(1,3)}{2} \end{vmatrix} \tag{9}$$

2. The second condition, if i_x is a fraction and i_y is integer, then the pixel in the element matrix w_{22} window is shown as Equation (10).

$$w_{22}(i,j) = \begin{vmatrix} w_{33}(2,2) & \dfrac{w_{33}(2,3)+w_{33}(3,3)}{2} \\ w_{33}(3,2) & \dfrac{w_{33}(2,1)+w_{33}(3,1)}{2} \end{vmatrix} \tag{10}$$

3. The third condition, if i_x and i_y are fractions, then the pixel in the element matrix w_{22} window is shown as Equation (11).

$$w_{22}(i,j) = \begin{vmatrix} w_{33}(2,2) & w_{33}(2,3) \\ w_{33}(3,2) & w_{33}(3,3) \end{vmatrix} \tag{11}$$

3.3. **Window weight.** We design window weight ($w_w(i,j)$) with 2×2 window size such as that written in Equation (12). The element of window weight is obtained from linear curve in Figure 3. Figures 3(a) and 3(b) have two linear curves, and there are uphill curve and downhill curve.

$$w_w(i,j) = \begin{vmatrix} a_{11} & a_{12} \\ a_{21} & a_{22} \end{vmatrix} \tag{12}$$

wherein the element matrix $a_{ij} = w_{xi}w_{yj}$, with $i = j = 1, 2$. Meanwhile, w_{xi} and w_{yj} are the weight values based on the linear curve on Figure 3. The w_{x1} and w_{x2} values are obtained by using Equations (13) and (14).

$$w_{x1} = \frac{b - i_x}{b - a} \tag{13}$$

$$w_{x2} = \frac{i_x - a}{b - a} \tag{14}$$

wherein a value is obtained from rounding down of i_x and b value is obtained from rounding up of i_x.

Moreover, the w_{y1} and w_{y2} values are obtained by similar ways which are written in Equations (13) and (14). However, the i_x variable in both equations must be replaced by i_y variable.

3.4. **The filling pixel.** Finally, one pixel can be calculated using Equation (15). This pixel is used to fill the target image coordinate, shown in Figure 2. By repeating, starting from Equation (4) up to Equation (15), all element matrices of the target image can be filled by pixel.

$$f_T(x,y) = \sum_{i=1}^{2}\sum_{j=1}^{2} w_{22}(i,j)w_w(i,j) \tag{15}$$

4. **Experimental Result and Discussion.** In this experiment, we use seven test images, such as Lena, Boats, Baboon, Peppers, Butterfly, Zebra and Dolphin images as shown in Figure 4. The proposed method is compared with seven comparison methods, which are bilinear interpolation (BLI), bicubic interpolation (BCI), Lanczos interpolation (LI), new edge directed interpolation (NEDI) [11], reverse diffusion interpolation (RDI) [10], weighted linear extrapolation (WLE) [9] and pyramid step enlargement (PS) [19].

4.1. **Experimental result.** We use the source images in different sizes. Those are Lena (128×128), Boats (175×143), Baboon (128×128), Peppers (128×96), Butterfly (150×94), Zebra (220×140) and Dolphin (128×102). All methods are used to enlarge the source images by using a scale factor equal to four. The size of image enlargement results for Lena, Boats, Baboon, Peppers, Butterfly, Zebra and Dolphin images are 512×512, 700×572, 512×512, 512×384, 600×376, 880×560 and 512×408 respectively.

Four experiments are conducted in the proposed work. The first experiment is to calculate the peak signal-to-noise ratio (PSNR), correlation value and computation time result for image enlargement by a scale factor equal to four. Here, we use all the image tests on Figure 4 as the object experiment. The third results (PSNR, correlation value and computation time) are presented in Table 1 up to Table 3. The second experiment is to show the performance of the image enlargement method on the scale factor equal to four. In this case, we use Zebra image in Figure 4(f) as a sample test image. The image enlargement result is presented in Figure 5. The third experiment is to analyze the visual performance of image enlargement in different ratios using PWK method. We use Dolphin image (Figure 4(g)) as the sample test image. The image enlargement result is shown in Figure 6. Figure 6(a) is the source image and the target image size. Figure 6(b) is image enlargement result using PWK. Figure 6(c) is the source image with manual area selection. Meanwhile, Figure 6(d) is the image enlargement result using PWK based on

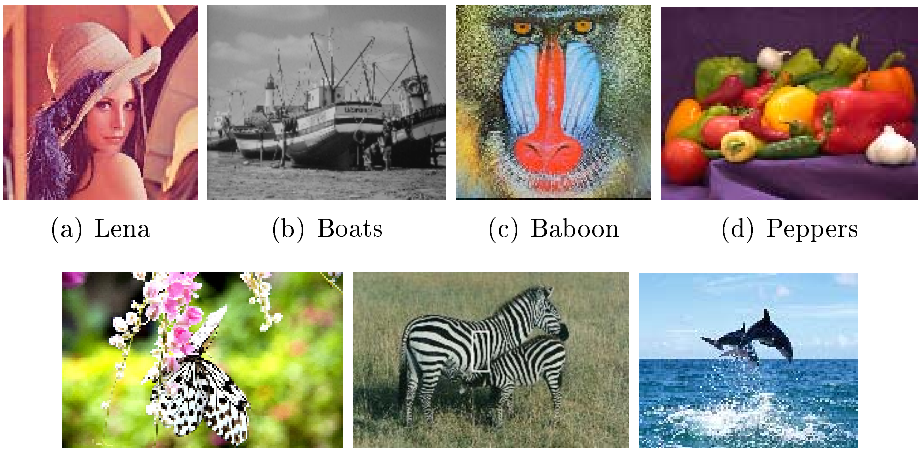
(a) Lena (b) Boats (c) Baboon (d) Peppers

(e) Butterfly (f) Zebra (g) Dolphin

FIGURE 4. Test images

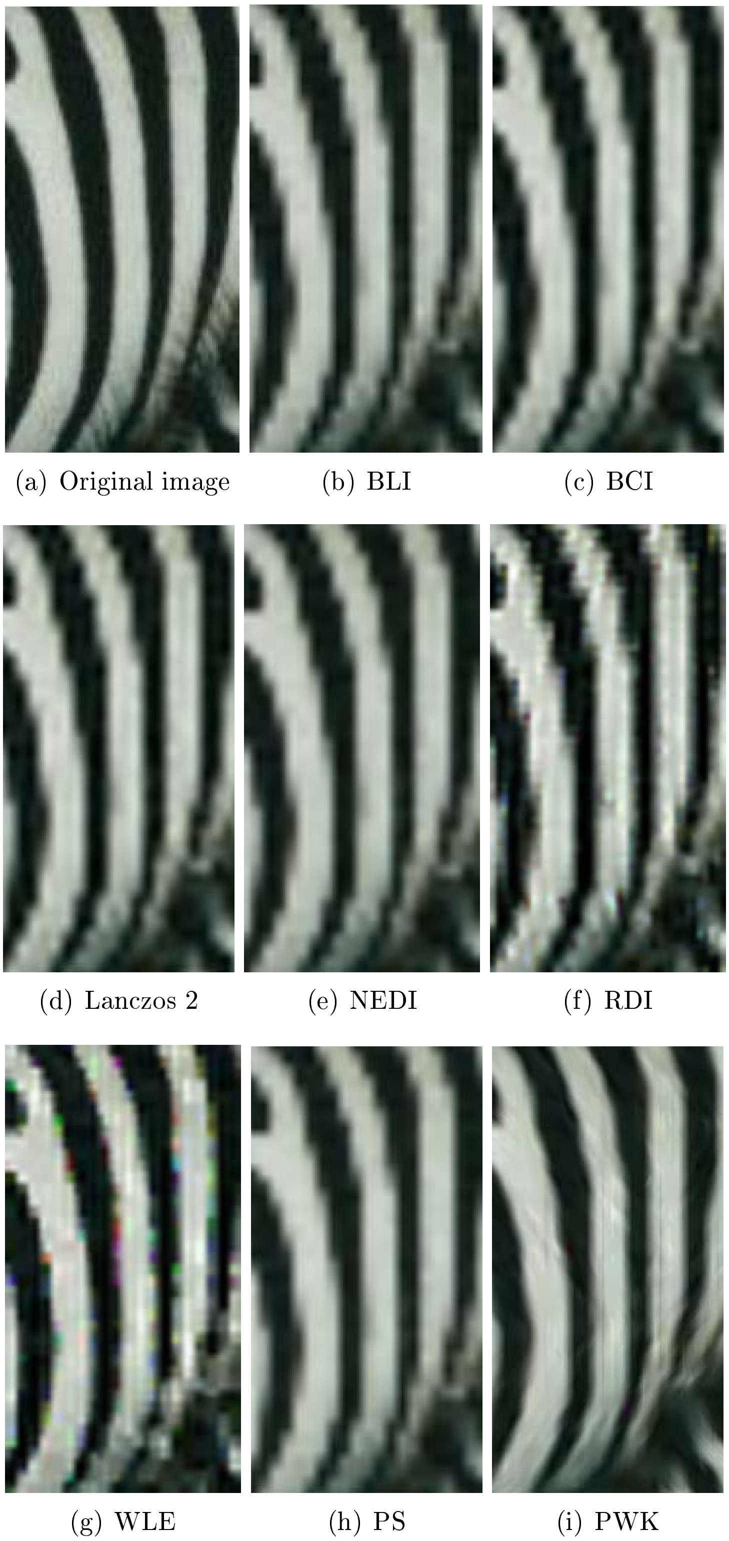

(a) Original image (b) BLI (c) BCI

(d) Lanczos 2 (e) NEDI (f) RDI

(g) WLE (h) PS (i) PWK

Figure 5. The original Zebra image cropped and the image enlargement results on scale factor $S = 4$

area selection. The fourth experiment is to show the visual result of image enlargement to the different shapes of a target image size that is presented in Figure 7. Figures 7(a) and 7(c) present the source image size with trapezoid and oval target image size

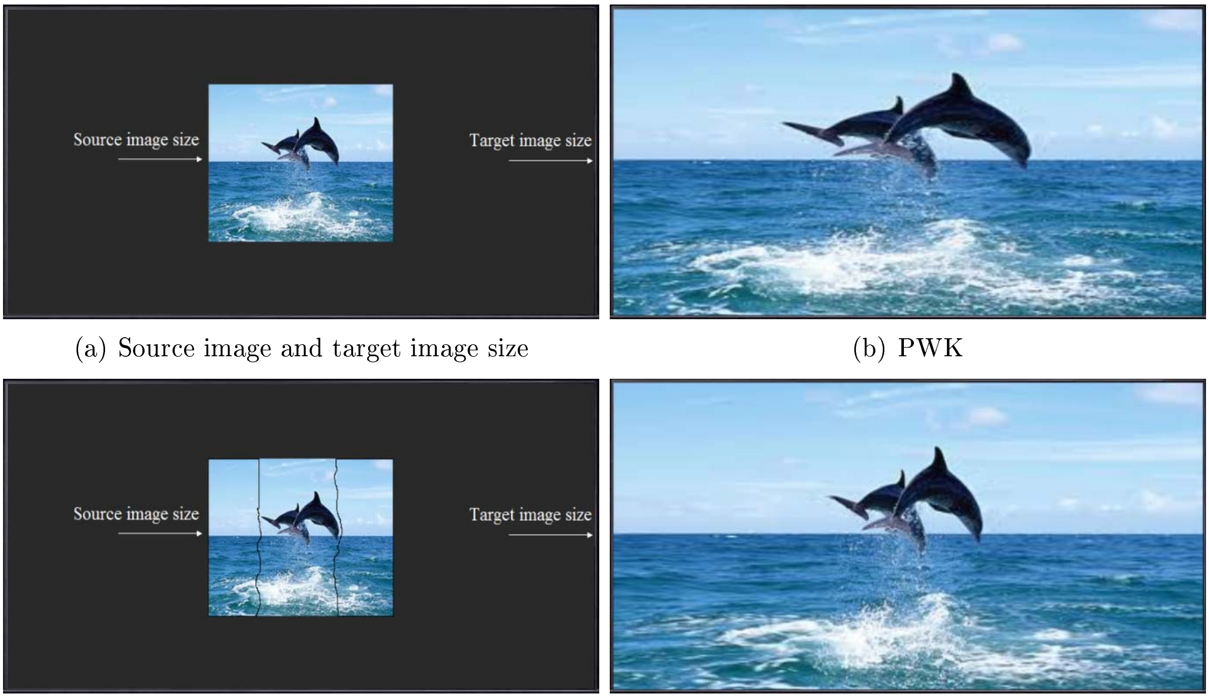

(a) Source image and target image size

(b) PWK

(c) Source image with selection area and target image size

(d) PWK based on image selection

Figure 6. Image enlargement in different ratio

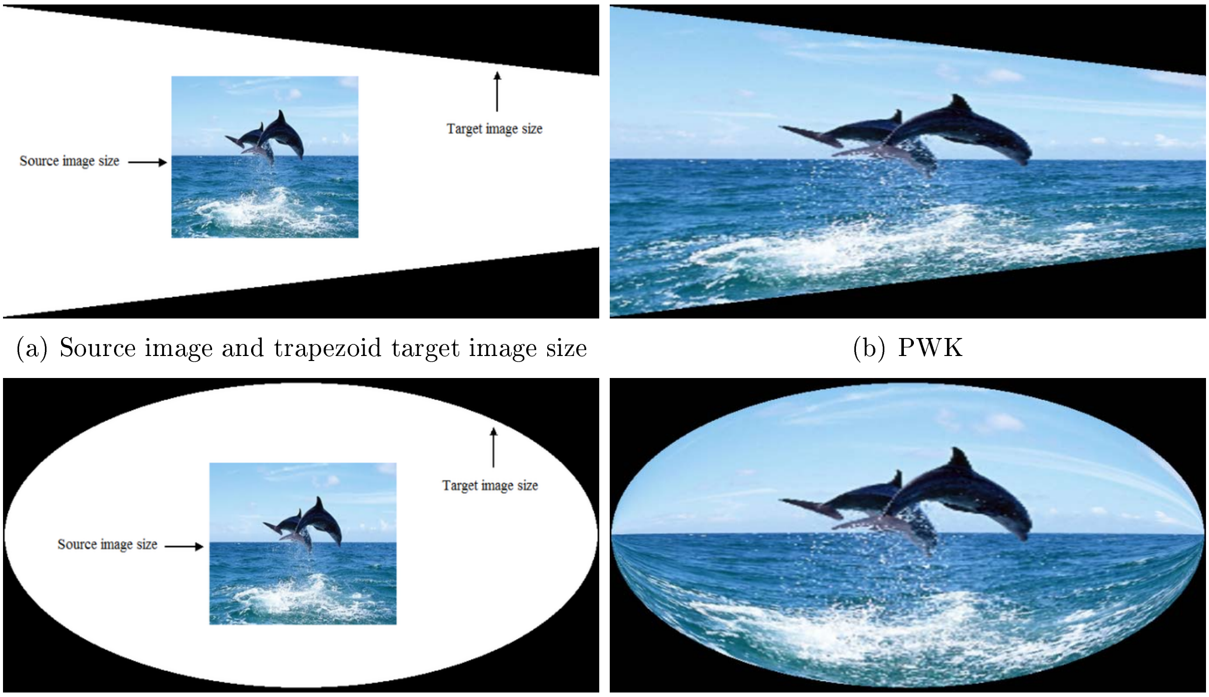

(a) Source image and trapezoid target image size

(b) PWK

(c) Source image and oval target image size

(d) PWK

Figure 7. Image enlargement to the different shapes of target image size

respectively. Furthermore, Figures 7(b) and 7(d) are the image enlargement results using PWK method.

4.2. **Evaluation method.** The quality of the enlargement image is evaluated by using quantitative and qualitative evaluation. The information about these evaluations is explained in subsubsections below.

4.2.1. *Quantitative evaluation.* We use peak signal-to-noise ratio (PSNR), correlation values and computation time for quantitative evaluation. Image evaluation by using PSNR and correlation values are required two images with similar size. The first image is a reference image and the second image is the enlarged image result. For this purpose, we create a scenario to test them using PSNR and correlation values as follows. Firstly, we provide a reference image. Next, we resize it into the smaller size. The sizes of images which would be enlarged is $^1/_4$ of their original size. The next step is to re-enlarge the smaller image sizes into their original sizes with scale factor $S = 4$. Thus, we are able to evaluate the quality of enlargement result using PSNR and correlation value. The third evaluation is explained in the following side.

1. The first mathematical evaluation uses PSNR as shown in Equation (16).

$$PSNR = 10 \log \frac{MN\max(f(x,y))}{\sum_{y=1}^{M}\sum_{x=1}^{N}\left(f(x,y) - f_T(x,y)\right)^2} \tag{16}$$

wherein $f(x,y)$ is reference image and $f_T(x,y)$ is the image enlargement result.

Table 1 shows PSNR values for image enlargement by scale factor equal to four on images Lena, Boats, Baboon, Peppers, Butterfly, Zebra and Dolphin. In this evaluation, the PSNR value of PWK has the highest PSNR value compared with seven comparison methods such as BLI, BCI, Lanczos 2, NEDI, RDI, WLE and PS. The highest PSNR value indicates better image quality.

2. The second evaluation uses correlation value between the reference images and the enlargement image result as shown in Equation (17).

$$r = \frac{\sum_{y=1}^{M}\sum_{x=1}^{N}\left(f(x,y) - \overline{f}\right)\left(f_T(x,y) - \overline{f_T}\right)}{\sqrt{AB}} \tag{17}$$

$$A = \sum_{y=1}^{M}\sum_{x=1}^{N}\left(f(x,y) - \overline{f}\right)^2 \tag{18}$$

$$B = \sum_{y=1}^{M}\sum_{x=1}^{N}\left(f_T(x,y) - \overline{f_T}\right)^2 \tag{19}$$

wherein $\overline{f}$ is equal to the mean value of $f(x,y)$ and $\overline{f_T}$ is equal to the mean value of $f_T(x,y)$.

Correlation evaluation is used to measure the power of two variables. The two variables are referencing image and the enlargement image result. The power of two variables is expressed by values between 0 to 1. If the value of the correlation is close to 1, then the $f_o(x,y)$ is very similar with image reference and vice versa.

The evaluation result using correlation value is shown in Table 2. On test images Lena and Boat only NEDI has the correlation value less than 0.9, whereas other methods have the correlation values greater than 0.9. The correlation evaluation shows PWK method always has the correlation values higher than the comparison method.

3. We use computers with specification Intel Core (TM) 2.9 GHz CPU, 4 GB RAM. All the methods are implemented in Matlab 7.5.0 R2007b. Table 3 shows the computation time for NEDI, RDI, WLE, PS and PWK. The computation time of PWK is faster than NEDI, RDI, WLE and PS.

Table 1. PSNR for image enlargement by $S = 4$

Method	Image samples						
	Lena	Boats	Baboon	Papper	Butterfly	Zebra	Dolphin
Bilinear	24.01	22.87	19.09	25.34	17.69	19.27	18.79
Bicubic	23.58	22.47	18.54	25.01	17.26	18.84	18.22
Lanczos 2	23.57	22.45	18.53	25.00	17.25	18.83	18.21
NEDI [11]	20.38	19.77	17.85	21.20	15.12	16.13	17.35
RDI [10]	23.32	22.28	18.44	24.79	17.13	18.67	18.15
WLE [9]	24.43	22.81	18.53	26.00	17.15	18.22	18.18
PS [19]	27.07	25.12	19.92	28.48	19.24	21.32	19.69
PWK	27.43	25.52	20.43	29.58	19.97	21.56	19.76

Table 2. Correlation value for image enlargement by $S = 4$

Method	Image samples						
	Lena	Boats	Baboon	Papper	Butterfly	Zebra	Dolphin
Bilinear	0.946	0.942	0.864	0.978	0.890	0.844	0.872
Bicubic	0.946	0.937	0.850	0.977	0.881	0.8337	0.858
Lanczos 2	0.941	0.936	0.849	0976	0.881	0.8334	0.857
NEDI [11]	0.878	0.881	0.823	0.944	0.799	0.685	0.825
RDI [10]	0.938	0.934	0.847	0.975	0.878	0.829	0.856
WLE [9]	0.955	0.944	0.855	0.982	0.887	0.835	0.861
PS [19]	0.975	0.967	0.889	0.990	0.925	0.906	0.899
PWK	0.976	0.969	0.900	0.992	0.936	0.911	0.899

Table 3. Computation time (second) for image enlargement by $S = 4$

Method	Image samples						
	Lena	Boats	Baboon	Papper	Butterfly	Zebra	Dolphin
NEDI [11]	18.783	28.485	20.389	13.447	47.944	111.68	46.145
RDI [10]	37.689	51.636	37.971	28.080	90.871	181.67	88.874
WLE [9]	1.419	2.199	1.435	0.982	3.369	8.029	3.229
PS [19]	1.154	1.645	1.139	0.796	2.075	5.530	1.981
PWK	1.014	1.560	1.029	0.686	2.043	4.960	1.888

4.2.2. *Qualitative evaluation.* To evaluate the visual quality result of several image enlargement methods, we show the cropping of Zebra image, especially in the stomach area that is illustrated in the mark a square line as shown in Figure 4(f). The cropping of Zebra image enlargement results by a scale factor equal to fours as shown in Figure 5(b) up to Figure 5(i).

Comparison method for BLI, BCI and Lanczos 2 in Figure 5(b) up to Figure 5(d) look rough texture. The NEDI method in Figure 5(e) looks a good quality in the edge of image areas. RDI and WLE methods produce a jagged image enlargement, especially in edge areas as shown in Figures 5(f) and 5(g). Figures 5(h) and 5(i) are the image enlargement results by using PS and PWK methods respectively. Both of images look similar. However, the PS method is slightly more blurry compared with PWK method.

4.3. **Discussion.** The computation time of PWK is faster than those of the fastest image enlargement methods such as WLE, NEDI and PS. In addition, PWK has a good image quality. PWK method is very easy to implement in hardware, because this method does not require complex calculations. However, for the real-time image enlargement, the faster hardware is needed.

In software implementation, PWK method is used for video rendering. There are three steps in the implementation of PWK methods for video rendering. First, video is converted into the frames and then frames into images. Second, the PWK method is applied to enlarging the images which are separated from the frames. For example, the source image Dolphin (408×512) is enlarged to become the target image size (1080×2048). Target image size is 2K display with a ratio 9:17. The image enlargement result is shown in Figure 6(b). Third, after the frame enlargement process, the enlarged frames are converted back to the movie.

PWK method is applied to the proportional content image enlargement. In this case, we select three regions from the source image manually as shown in Figure 6(c), and then, we enlarge the source image by same scale factor value for the S_h and S_w. The scale factor value for S_h and S_w is equal to scale factor value for height, which is calculated from height size of source image and the target image. The result is placed in the center of target image size. Furthermore, we enlarge the left and right regions of selected image to obtain full image size. In this step, the scale factor for S_h is equal to one. Whereas, the scale factor for S_w is always changing following the image area selection. So that, the scale factor for the S_w must be calculated in each row. By different scale factor value for S_w, we obtain the proportional image enlargement in different ratios as shown in Figure 6(d).

We demonstrate two examples image enlargement in different shapes by using PWK method. Image resizing in different shapes usually used to design animation effect. Figures 7(a) and 7(c) show the size of each row and column of the target image always changing. That affects the changing of the scale factor on each row and column. This problem can be solved by counting the scale factor in each coordinate pixel that will be filled with Equations (2) and (3). Furthermore, the filling process of one pixel value in every target image coordinates can be calculated by using Equation (2) up to Equation (15). This process is repeated until all the coordinates on target image have been filled by pixel. Both results are shown in Figures 7(b) and 7(d) for trapezoid and oval shapes respectively.

The example of image enlargement on Figures 7(b) and 7(d) prove that the PWK method has flexibility, because it can be used to enlarge the image in the different shapes. Both examples have represented the varying shape of target image. PWK method based on the filling pixels will be easily implemented in the image retargeting. Image retargeting is changing the image size at the different ratios. If we look at Figure 7(d), the height of the target image size on the left and right side is lower than the source image. Meanwhile, the center of image has a higher size than the source image. In this case, it has proven that PWK method is capable of handling image enlargement in many variation heights or widths of the target image size.

5. **Conclusions.** We introduce a new image enlargement method by combining pyramid method and linear curve. We call it as PWK method. The proposed method has been tested on Lena, Boats, Baboon, Peppers, Butterfly, Zebra and Dolphin images. The evaluation results of image enlargement using PNSR and correlation value have been presented. Referring from two evaluations, the image enlargement using PWK method has a good image quality. The computation time of PWK method is faster than comparison

methods. The PWK method is very easy to implement on image enlargement in different ratios and shapes of target image size.

For the next study, we will develop the selection image enlargement by combining PWK method with an image feature detection. The method aim is to create an image enlargement method with the feature content maintaining.

Acknowledgment. The authors would like to thank the Directorate General of Higher Education Ministry of National Education (DGHE) of Indonesia, which provides scholarship.

REFERENCES

[1] H. Tamukoh, H. Kawano, N. Suetake, B. Cha and T. Aso, Fast image-enlargement algorithm for the augmentation of the high-frequency component by employing a hierarchical predefined codebook, *International Journal of Innovation Computing, Information and Control*, vol.9, no.2, pp.903-914, 2013.

[2] C. Liu and X. Luo, Image enlargement via interpolatory subdivision, *IET Image Processing*, vol.5, no.6, pp.568-571, 2011.

[3] D. Park, K. Lee and Y. Kim, Real-time processing technique for content-aware image resizing of video, *International Journal of Innovation Computing, Information and Control*, vol.9, no.4, pp.1477-1492, 2013.

[4] C. Chen, H. Y. Lin and C. H. Hsieh, Novel stereo image and video retargeting approach, *International Journal of Innovation Computing, Information and Control*, vol.9, no.4, pp.1727-1736, 2013.

[5] Y. Gou, F. Liu, J. Shi, Z. H. Zhou and M. Gleicher, Image retargeting using mesh parametrization, *IEEE Trans. on Multimedia*, vol.11, no.5, 2009.

[6] S. Sugimoto, S. Shimizu, H. Kimata and A. Kojima, Multi-layer image retargeting, *International Conference on Image Processing*, pp.3001-3004, 2012.

[7] S. Salehi and H. Mahdavi-Nasab, New image interpolation algorithms based on dual-tree complex wavelet transform and multilayer feedforward neural networks, *International Journal of Innovation Computing, Information and Control*, vol.8, no.10(A), pp.6885-6902, 2012.

[8] H. C. Chen and W. J. Wang, Locally edge-adapted distance for image interpolation based on genetic fuzzy system, *Expert System with Applications*, vol.37, pp.288-297, 2010.

[9] T. Aso, N. Sutake and T. Yamakau, A fast and accurate image enlargement algorithm employing a weighted sum of linear extrapolations, *Automation Congress, Proceedings*, vol.18, pp.251-258, 2004.

[10] O. Salvado, C. M. Hillenbrand and D. L. Wilson, Partial volume reduction by interpolation with reverse diffusion, *International Journal of Biomedical Imaging*, vol.2006, pp.1-13, 2006.

[11] X. Li and M. P. Orchard, New edge-directed interpolation, *IEEE Trans. on Image Processing*, vol.10, pp.1521-1527, 2001.

[12] Y. Y. Liu, M. Chen, H. Ishikawa, G. Wollstein, J. S. Schuman and J. M. Rehg, Automated macular pathology diagnosis in retinal OCT images usingmulti-scale spatial pyramid and local binary patterns in texture and shape encoding, *Medical Image Analysis*, vol.15, pp.748-759, 2011.

[13] G. Borgefors, G. Ramella and G. S. di Baja, Shape and topology preserving multi-valued image pyramids for multi-resolution skeletonization, *Pattern Recognition Letters*, vol.22, pp.741-751, 2001.

[14] T. M. Chan, J. Zhang, J. Pu and H. Huang, Neighbour embedding based super-resolution algorithm through edge detection and feature selection, *Pattern Recognition Letters*, vol.30, pp.494-502, 2009.

[15] M. V. Joshi, S. Chaudhuri and R. Panuganti, Super-resolution imaging: Use of zoom as a cue, *Image and Vision Computing*, vol.22, pp.1185-1196, 2004.

[16] K. Petra, J. Benois-Pineau and J. P. Domenger, Local object-based super-resolution mosaicing from low-resolution video, *Signal Processing*, vol.91, pp.1771-1780, 2011.

[17] G. Flouzat, O. Amram, F. Laporterie and S. Cherchali, Multiresolution analysis andreconstruction by a morphological pyramidin the remote sensing of terrestrial surfaces, *Signal Processing*, vol.81, pp.2171-2185, 2001.

[18] H. C. Chen and W. J. Wang, Fuzzy-adapted linear interpolation algorithm for image zooming, *Signal Processing*, vol.89, pp.2490-2502, 2009.

[19] I. K. Somawirata, K. Uchimura and G. Koutaki, Enlargement digital image by pyramid steps algorithm with local image data, *Proc. of the 18th Korea-Japan Join Workshop on Frontiers of Computer Vision*, pp.153-159, 2012.